Precise control of environmental factors reduces variability in scopolamine-induced murine dry-eye model

Keefe, Madeleine PhD[1]; Moody, Kelsey PhD[2]; Kirkgasser, Katherine BS[2]; Sargrad, Andrew BS[2]; Grohn, Kris PhD[2]; Davis, Mallory MS[2]

1. BioSpherix, LLC (25 Union Street, Parish, NY | sales@biospherix.com); 2. Ichor Life Sciences, Inc. (2561 US-11, Lafayette, NY | info@ichorlifesciences.com

Poster #3919

Background

Murine models combining scopolamine administration and desiccating stress have been utilized extensively in dry eye research. However, the robustness and reproducibility of these models is often compromised by homemade housing systems that do not tightly regulate environmental factors such as humidity and temperature. In the present study, we characterized and validated the BioSpherix® Dry Eye System for this application.

Methods

Study design:
- Female C57BL/6 mice (8 weeks old)
- Groups: Naïve (n = 5, 10 eyes) and Dry Eye Disease (DED; n = 15, 30 eyes)

Dry Eye Induction
- Scopolamine hydrobromide (2.5 mg/mL), subcutaneous
- 4x daily 0.5 mg/dose (08:00, 11:00, 14:00, 17:00)

Environmental Control by BioSpherix Dry Eye System*
- Humidity: ≤30% via clean, dry air (CDA) and optional desiccant
- Custom BioSpherix cages provided 8 cfm airflow
- Temperature: 26°C

In-Life Assessments
- Corneal Imaging
  - 0.6 µL 0.75% fluorescein sodium applied to cornea (t=0 minutes)
  - Mice anesthetized using inhalant anesthesia (t=10 minutes)
  - Images captured with the Phoenix Micron IV slit lamp system with cobalt blue excitation (t=12 minutes)
- Corneal Epithelial Defect
  - Images assessed by masked examiner using the NEI density grading system and by auto quantification of pixel count
- Tear Production Quantification
  - Phenol red-impregnated cotton thread placed in the medial canthus for 10 seconds
  - Tear volume quantified by length of color change (mm)

Tissue Analysis
- Tissue Collection
  - Timepoints: Days 2, 7, and 14
  - Eyes enucleated and corneas isolated
  - Flash frozen in liquid nitrogen, stored at -80°C

Molecular Analysis
- Proteomics via Orbitrap Astral mass spectrometry
- Data deposited into the Ichor Differential Expression Atlas (IDEA)

*BioSpherix Dry Eye System

Results

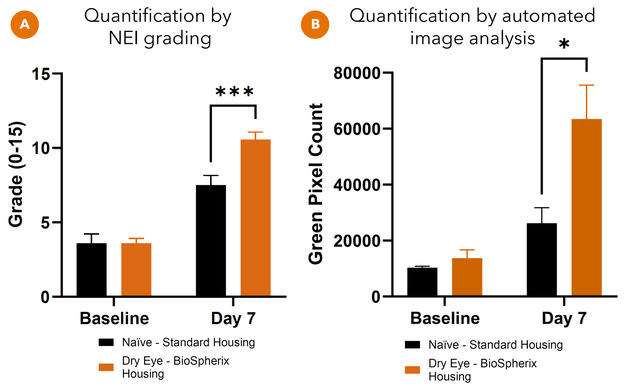

Fig 1: Corneal fluorescein stain quantification after dry-eye induction

Corneal surface punctate stain assessed and quantified using **A.** NEI grading and **B.** automated image analysis with epithelial defect area determined by pixel count. Corneal surface punctate staining was assessed at baseline and Day 7 post-induction. Dry eye induction resulted in an increase in corneal punctate density by Day 7 relative to baseline and naïve controls (*p < 0.05, **p< 0.01, ***p < 0.001, ****p < 0.0001). Pairwise comparisons not reaching significance were excluded.

Fig 2: Tear volume assessment following dry eye induction (Phenol-Red Thread Test)

A reduction in tear volume was observed in the DED group at Day 7 relative to baseline and naïve controls. (*p < 0.05, **p < 0.01, ***p < 0.001, ****p < 0.0001). Pairwise comparisons not reaching significance were excluded from analysis.

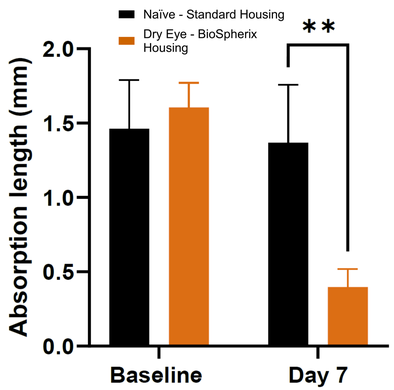

Fig 3: Daily relative humidity profiles across housing settings

A. Daily mean relative humidity was recorded in three environments: the Dry Eye System chamber, the cage within the Dry Eye chamber, and standard ambient housing. Desiccation housing maintained consistently lower, stable humidity compared to ambient conditions.

B. Technician performing animal handling within BioSpherix Dry Eye chamber.

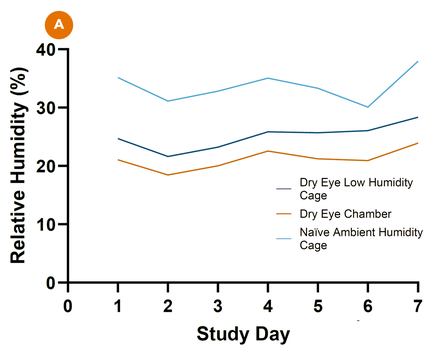

Fig 4: Top differentially expressed proteins following dry eye induction

A. Top up- and down-regulated proteins ranked by fold change. **B.** Volcano plot of differentially expressed proteins between treatment groups.

A

Gene	Protein Name	Log_2 Fold Change	P-Value	Function
Upregulated Proteins				
Eln	Elastin	6.93	4.95E-03	Extracellular matrix elasticity; tissue remodeling under stress
Crygc	Gamma-crystallin C	5.64	3.79E-02	Structural protein; maintains stability under stress
Crygf	Gamma-crystallin F	5.58	5.85E-02	Prevents aggregation; supports protein stability
Crygb	Gamma-crystallin B	5.06	3.34E-02	Maintains structural integrity during cellular stress
Crygs	Gamma-crystallin S	4.98	2.02E-02	Cytoprotective; protects against oxidative stress
Crygd	Gamma-crystallin D	4.95	4.68E-02	Stabilizes proteins under desiccation and oxidative stress
Crybb2	Beta-crystallin B2	4.51	9.72E-02	Maintains protein structure and cellular homeostasis
Cryba4	Beta-crystallin A4	4.48	1.37E-01	Structural stability; stress-responsive protein maintenance
Igkv4-63	Immunoglobulin kappa variable 4-63	4.42	9.83E-03	B-cell activation; adaptive immune response marker
Ighv10-1	Immunoglobulin heavy variable 10-1 (Fragment)	4.34	2.60E-01	Antigen-driven immune activation; inflammation-associated
Downregulated Proteins				
Bicdl1	BICD family-like cargo adapter 1	-8.07	5.39E-03	Intracellular transport; supports stress adaptation mechanisms
F8	Coagulation factor VIII	-5.81	1.79E-03	Coagulation factor; reflects injury and inflammation response
CK137956	cDNA sequence CK137956	-5.65	1.65E-02	Uncharacterized transcript; potential stress response role
Cdsn	Corneodesmosin	-5.06	1.18E-02	Epithelial barrier integrity; desiccation stress response
Slc25a31	ADP/ATP translocase 4	-4.16	1.17E-02	Mitochondrial transport; supports cellular energy metabolism
Ighv1-42	Immunoglobulin heavy variable V1-42	-4.12	3.47E-01	Adaptive immune activation; inflammation-associated marker
Stk19	Serine/threonine-protein kinase 19	-4.02	6.57E-03	Kinase signaling; regulates stress and inflammation pathways
Timm13	Mitochondrial import inner membrane translocase subunit Tim13	-3.94	8.11E-03	Mitochondrial protein import; supports stress resilience
Tmem132a	Transmembrane protein 132A	-3.73	3.97E-02	Cell adhesion; potential stress signaling involvement
Golt1b	Vesicle transport protein GOT1B	-3.63	3.34E-02	Golgi transport; supports protein processing under stress

B

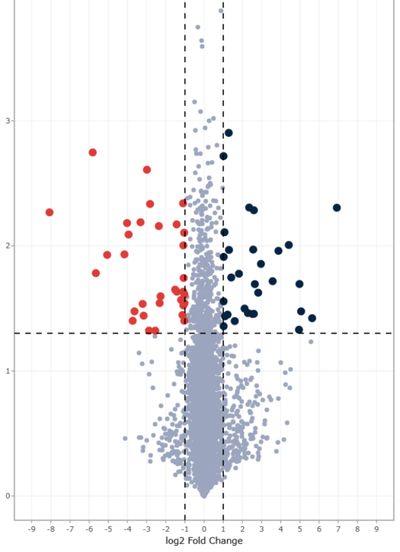

Conclusions

- Functional (tear volume), structural (corneal epithelial defect), and molecular (proteomic) changes confirm successful disease induction using the BioSpherix Dry Eye System in the murine dry-eye model.
- Temporal molecular characterization by unbiased proteomics enables investigators to query for the presence of targets of interest through Ichor Differential Expression Atlas (IDEA) and select dosing strategies informed by optimal target expression.

References

1. Chen, Y., Chauhan, S. K., Lee, H. S., Stevenson, W., Schaumburg, C. S., Sadrai, Z., Saban, D. R., Kodati, S., Stern, M. E., & Dana, R. (2013). Effect of desiccating environmental stress versus systemic muscarinic achr blockade on dry eye immunopathogenesis. Investigative Opthalmology & Visual Science, 54(4), 2457. https://doi.org/10.1167/iovs.12-11121
2. Yu, Z., Yazdanpanah, G., Alam, J., De Paiva, C. S., & Pflugfelder, S. (2023). Induction of innate inflammatory pathways in the corneal epithelium in the desiccating stress dry eye model. Investigative Opthalmology & Visual Science, 64(4), 8. https://doi.org/10.1167/iovs.64.4.8

Conflict of Interest Disclosure: Authors are employees of BioSpherix, LLC and Ichor Life Sciences, Inc.